frontiers | Frontiers in Plant Science

ORIGINAL RESEARCH
published: 25 April 2022
doi: 10.3389/fpls.2022.873065

Optical Property Mapping of Apples and the Relationship With Quality Properties

Hehuan Peng[1], Chang Zhang[2], Zhizhong Sun[3], Tong Sun[1], Dong Hu[1], Zidong Yang[1] and Jinshuang Wang[4]*

[1] College of Optical, Mechanical and Electrical Engineering, Zhejiang A&F University, Hangzhou, China, [2] Office of Educational Administration, Zhejiang A&F University, Hangzhou, China, [3] College of Mathematics and Computer Science, Zhejiang A&F University, Hangzhou, China, [4] Key Laboratory of Crop Harvesting Equipment Technology of Zhejiang Province, Jinhua, China

This paper reports on the measurement of optical property mapping of apples at the wavelengths of 460, 527, 630, and 710 nm using spatial-frequency domain imaging (SFDI) technique, for assessing the soluble solid content (SSC), firmness, and color parameters. A laboratory-based multispectral SFDI system was developed for acquiring SFDI of 140 "Golden Delicious" apples, from which absorption coefficient (μ_a) and reduced scattering coefficient (μ_s') mappings were quantitatively determined using the three-phase demodulation coupled with curve-fitting method. There was no noticeable spatial variation in the optical property mapping based on the resulting effect of different sizes of the region of interest (ROI) on the average optical properties. Support vector machine (SVM), multiple linear regression (MLR), and partial least square (PLS) models were developed based on μ_a, μ_s' and their combinations ($\mu_a \times \mu_s'$ and μ_{eff}) for predicting apple qualities, among which SVM outperformed the best. Better prediction results for quality parameters based on the μ_a were observed than those based on the μ_s', and the combinations further improved the prediction performance, compared to the individual μ_a or μ_s'. The best prediction models for SSC and firmness parameters [slope, flesh firmness (FF), and maximum force (Max.F)] were achieved based on the $\mu_a \times \mu_s'$, whereas those for color parameters of b* and C* were based on the μ_{eff}, with the correlation coefficients of prediction as 0.66, 0.68, 0.73, 0.79, 0.86, and 0.86, respectively.

Keywords: optical property mapping, spatial-frequency domain imaging, apple, quality, correlation, prediction

OPEN ACCESS

Edited by:
Jiangbo Li,
Beijing Academy of Agriculture and Forestry Sciences, China

Reviewed by:
Yanru Zhao,
Northwest A&F University, China
Xiongzhe Han,
Kangwon National University, South Korea

***Correspondence:**
Dong Hu
20180047@zafu.edu.cn

Specialty section:
This article was submitted to Crop and Product Physiology, a section of the journal Frontiers in Plant Science

Received: *10 February 2022*
Accepted: *03 March 2022*
Published: *25 April 2022*

Citation:
Peng H, Zhang C, Sun Z, Sun T, Hu D, Yang Z and Wang J (2022) Optical Property Mapping of Apples and the Relationship With Quality Properties. Front. Plant Sci. 13:873065. doi: 10.3389/fpls.2022.873065

INTRODUCTION

The apple, famous for its rich vitamin and mineral with high-nutritional value, is one of the most consumed fruits worldwide. Apples are available throughout the year due to the advanced and strict storage control. After harvesting, apples are transported immediately from the orchard to the shed storage. Alternatively, apples are graded and sorted first in the warehouse, after which they are directly moved to the cold shed storage (Zhang et al., 2020, 2021). The latter case is more popular because it can meet the increasing and diverse demands of consumers for apple quality. Quality evaluation on intact apple fruit, which is the key step in the process of grading and sorting, is gaining tremendous interest and attention in the field of non-destructive inspection. In the past decades, visible and near-infrared (Vis/NIR) spectroscopy has been widely developed and adopted

for quality assessment of plant and food products (Zhao et al., 2020; Daniels et al., 2021; Li and Zhang, 2021; van Wyngaard et al., 2021; Wan et al., 2021), thanks to its rapid and non-invasive character. A large number of statistical models based on Vis/NIR spectroscopy have been built for predicting apple quality properties, such as firmness, crispness, soluble solid content (SSC), and acidity (Gao et al., 2016; Fan et al., 2020; Huang et al., 2020; Tian et al., 2020). However, these models are often valid for the conditions under which they were trained and are not applicable under very variable conditions, such as different cultivars, batches, and places of origin. The main reason causing the weak robustness and applicability of the statistical models is that conventional Vis/NIR spectroscopy typically relates the spectra to the chemical and/or physical properties using a "black-box" method directly and it cannot offer separate information on the absorption and scattering properties of plant and food tissues. It is thus desirable to reveal the insight into light-tissue interaction (mainly absorption and multiple scattering), which is expected to provide more reliable prediction of quality properties under very variable conditions.

In the last decade, optical properties of fruits and vegetables, mainly referring to absorption coefficient (μ_a, mm^{-1}) and reduced scattering coefficient (μ_s', mm^{-1}), have been measured by different researchers using diverse optical sensing techniques (Hu et al., 2015; Lu et al., 2020), such as integrating sphere (IS), time-resolved (TR), spatially resolved (SR) and spatial-frequency domain imaging (SFDI). Sun C. et al. (2020) used IS coupled with inverse adding-doubling algorithm for extracting the μ_a and μ_s' of citrus fruit. Huang et al. (2018) measured the μ_a and μ_s' of tomatoes at six maturity stages from multichannel hyperspectral imaging-based SR spectra. Vanoli et al. (2020) applied TR and SR spectroscopy to determine the μ_a and μ_s' of apples after ripening in shelf life. The measured optical properties were used for evaluating the physiochemical properties, such as water content, oil gland size, total soluble solids, titratable acidity, and firmness. All these studies are limited to point measurement, which means the measured optical property is from single point (usually one pixel), and it cannot attain the spatial distribution of optical properties through single measurement. Since plant and food tissues present heterogeneity to some extent, some researchers measured several tissue points and took the average value as the optical property (He et al., 2016). This attempt might partly weaken the effect of measurement location on the intrinsic optical property, but it could not address the issue fundamentally.

Spatial-frequency domain imaging, as an emerging modality for measuring optical properties, is capable of mapping μ_a and μ_s' on a pixel-by-pixel fashion, which enables to attain 2-D optical property distribution through single measurement. By demodulating the emitted images under structured illuminations with changed frequencies and phases, the μ_a and μ_s' can be estimated using inverse algorithm based on appropriate light transfer models (Hu et al., 2016). Owing to the capabilities of wide-field and non-contact imaging, and depth-varying and signal-enhanced characterization (Gigan, 2017), SFDI has been applied for measuring the optical property mappings of apple, kiwi, mango, and pear (Hu et al., 2020a; He et al., 2021; Lohner et al., 2021; Sun et al., 2021). However, no reports were found on the prediction of apple quality properties based on the measured optical property mappings. In addition, in the SFDI, one can extract the optical property of single pixel, as well as do the measurements of multiple pixels in a preselected ROI, but the results would present difference to some extent. It is thus necessary to quantify the effect of ROI size (i.e., number of pixels) on optical property measurement. Therefore, the objectives of this research were as (1) to measure the optical property (μ_a and μ_s') mappings of apples and compare the optical property difference among different sizes of ROI; (2) to relate the average optical properties to apple SSC, firmness, and color parameters; and (3) to evaluate prediction performance of apple quality properties based on the optical properties using different models.

MATERIALS AND METHODS

Apple Preparation

A total of 140 "Golden Delicious" apples with similar size and being free of visible defects were purchased from a local fruit supermarket at the city of Hangzhou. Physical properties (i.e., weight, diameter, and height) of the apples are measured and summarized in **Table 1**. To complete the acquisition of SFDI and the measurement of quality attributes for all the apples, the experiments were designed and conducted, with the flowchart shown in **Figure 1**. The intact apples were cut lengthwise to generate a slice with the thickness of about 15 mm. The slice (left in **Figure 1**) was used for juicing measurement to get the corresponding SSC value, while the other part (right in **Figure 1**) was subjected to the color measurement, SFDI measurement, and puncture test, respectively, from which the color parameters (L*, a*, b*, C*, and H°), optical property mapping, and firmness parameters [slope, flesh firmness (FF), and maximum force (Max.F)] were obtained. The measured optical property mapping was then used for data interpretation, correlation analysis, and quality prediction. During the experiment, apples were kept at room temperature (∼22°C) with no humidity control and the experiment was completed within 5 days.

Acquisition of Spatial-Frequency Domain Imaging and Optical Property Mapping

Spatial-frequency domain imaging of the apples was acquired using a laboratory-developed SFDI system, as shown in **Figure 2**. A detailed description of the SFDI system and its calibration procedure were given in our previous study (Hu et al., 2016). The SFDI system mainly consists of a light source, a digital projector, and a color camera. The light source, combined with the DLP-based projector, is used to generate structured patterns for illuminating the apples. The reflected light is received by the camera, which produces SFDI under different frequencies and phases. The neutral density filter mounted with the projector could reduce light intensity uniformly to avoid burning on the apples, while the bandpass filter placed in front of the camera is used for wavelength dispersion, constituting a multispectral SFDI system. A number of two crossed linear polarizers are mounted in the projection and detection arms to reduce specular reflection from the apple surface. In this study, four wavelengths of 460,

TABLE 1 | Statistics of physical and quality parameters for 140 "Golden Delicious" apples.

Test method	Parameter	Mean	*SD*	Max	Min	CV (%)
Auncel	Weight (g)	226.8	17.9	270.0	190	7.9
Vernier caliper	Diameter (mm)	80.4	2.4	84.9	74.9	2.9
	Height (mm)	68.0	3.7	77.4	59.4	5.4
	Slice thickness (mm)	14.8	0.9	17.2	12.1	5.6
Refractometer	SSC (%)	15.0	1.3	18.6	11.5	8.5
Puncture	Slope (N/mm)	7.3	1.7	11.1	3.4	22.9
	FF (N)	14.0	1.6	17.4	9.5	11.4
	Max.F (N)	16.7	1.2	19.8	13.6	17.5
Colorimeter	L*	76.8	1.1	79.2	74.1	1.4
	a*	−2.9	0.8	−1.1	−5.0	−7.8
	b*	27.3	1.8	34.3	22.6	10.2
	C*	27.4	1.8	34.6	22.8	10.2
	H°	96.1	1.7	100.0	92.4	1.7

SD, standard deviation; CV, coefficient of variation; FF, flesh firmness; Max.F, maximum force.

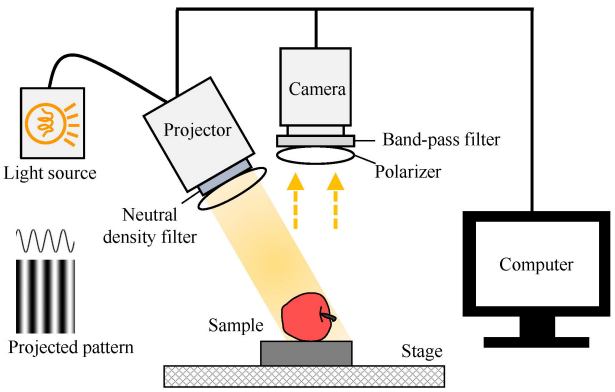

FIGURE 2 | Schematic of a multispectral spatial-frequency domain imaging system for measuring optical property mappings of apples.

527, 630, and 710 nm are used. When spatial frequency of the structured illumination is 0.20 mm^{-1}, the light penetration depth within apple tissue is approaching 1 mm (Hu et al., 2021). High-frequency illumination has a relatively shallow light penetration depth, which could be interpreted by the depth-varying feature (Hayakawa et al., 2018; Lu and Lu, 2019). To remove the effect of apple peel (with the thickness about 1 mm) on optical property mapping, six spatial frequencies with the values of 0, 0.04, 0.08, 0.12, 0.16, and 0.20 mm^{-1} were utilized in this study.

The captured SFDI of apples was processed using appropriate algorithms for extracting optical property mapping, among which image demodulation and inverse estimation are the two key steps (**Figure 3A**). Great efforts have been made to develop and improve the demodulation and inverse estimation methods (Lu et al., 2016; Hu et al., 2018, 2019; Sun et al., 2022). In this study, the conventional three-phase demodulation coupled with non-linear curve-fitting (TP-CF) method was applied for extracting optical property mapping of apples due to its high accuracy. To implement the TP-CF method, three-phase images at the same frequency were first demodulated to generate one alternative component (AC) image. Then, the non-linear curve-fitting method was used to extract the optical property (μ_a and μ_s') mappings of apples on a pixel-by-pixel fashion. It should be noted that two AC images are at least needed for curve fitting. The essential nature of the curve fitting is continuously iterative computing until the difference between the measured reflectance from the AC image and the computed reflectance based on the initially guessed optical properties is within the preset threshold

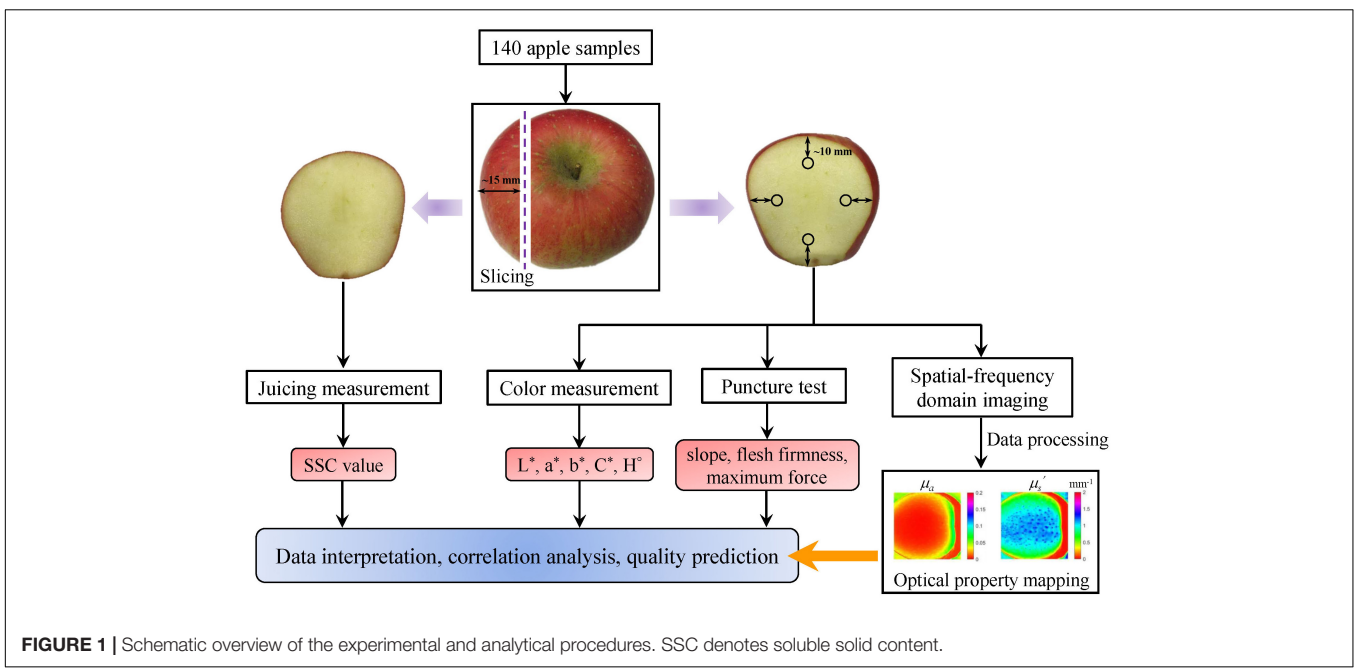

FIGURE 1 | Schematic overview of the experimental and analytical procedures. SSC denotes soluble solid content.

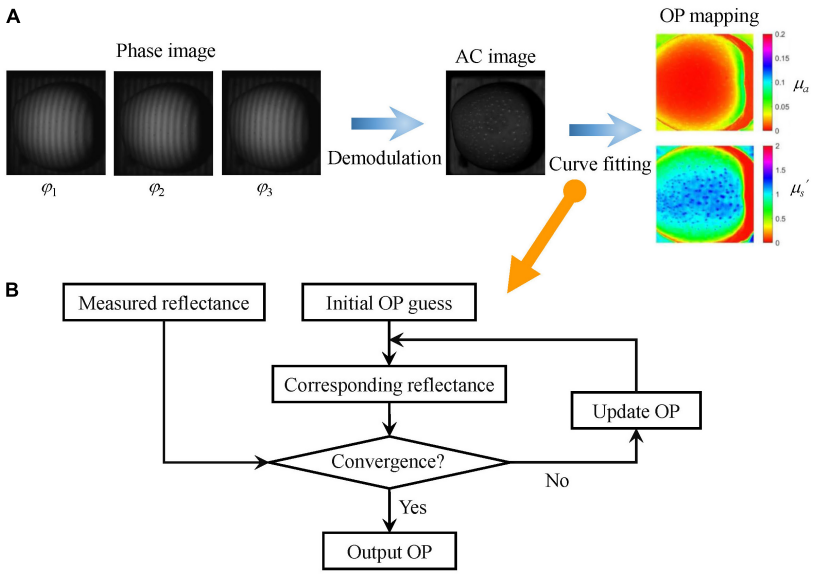

FIGURE 3 | Schematic of optical property mapping using three-phase demodulation coupled with curve fitting **(A)** and flowchart of the curve-fitting algorithm **(B)**. AC and OP denote alternative component and optical property, respectively.

(**Figure 3B**). In this occasion, dynamic adjustment is carried out to update the initial optical properties until the reflectance present a convergent pattern. To investigate the effect of ROI size on the optical property measurement, four ROIs with different sizes (i.e., 10 × 10, 30 × 30, 60 × 60, and 100 × 100 pixels, corresponding to 3 × 3 mm^2, 9 × 9 mm^2, 18 × 18 mm^2, and 30 × 30 mm^2 approximately) were selected, and the average value was taken as the optical property.

Measurement of Apple Quality Attributes

All the 140 apples were subjected to the measurement for different quality attributes. Juice of apple fruit was extracted from the apple slice (left in **Figure 1**), and SSC was measured using a handheld digital refractometer (model PR-101, Atago Co., Tokyo, Japan). Apple color was measured from the other part (right in **Figure 1**) using a colorimeter (CR-400, Konica Minolta Sensing, Inc., Tokyo, Japan) for the L*, a*, b*, C*, and H° values in triplicate, and average values were recorded for further analysis. As shown in **Figure 1**, apple firmness was measured from the surface area in quadruplicate with the distance between the center of puncture points and the external contour of apple about 10 mm, and the average values were recorded. Puncture tests were carried out using the texture analyzer (Model TA.XT plus, Stable Micro System, United Kingdom) equipped with a 5-mm cylindrical Magness-Taylor probe at a test speed of 4 mm/s and the penetration depth was set as 8 mm. A number of three parameters related to the firmness, which include slope in N/mm, FF in N, and Max.F in N, were then determined from the force–displacement curve. The slope was measured between the point of initial displacement and the point corresponding to the Max.F, while the FF was defined as the average force over the puncture distances between the rupture point and maximum puncture depth (8 mm).

Correlation Analysis and Prediction Modeling

Pearson's linear correlation analysis was performed on the relationship among all quality parameters and the absorption and reduced scattering coefficients as well as their combinations (i.e., μ_a, μ_s', $\mu_a \times \mu_s'$, and $\mu_{eff} = [3\mu_a\ (\mu_a + \mu_s')]^{1/2}$) using the software of IBM SPSS Statistics 25. $\mu_a \times \mu_s'$ is the multiplication of μ_a and μ_s', and it was reported to be more effective for predicting quality of tomatoes than using individual μ_a and μ_s' (Huang et al., 2018). μ_{eff} is a useful parameter for comparing light transmittance characteristics of different tissues and their wavelength dependence (Flock et al., 1987). To further explore the relationship between optical properties and quality parameters of apples (i.e., SSC, firmness and color), prediction models were established based on μ_a, μ_s', $\mu_a \times \mu_s'$, and μ_{eff} using support vector machine (SVM), multiple linear regression (MLR), and partial least squares (PLS) at the four wavelengths. The models of SVM, MLR, and PLS were developed by the Unscrambler X 10.4 software. All the 140 apple samples were randomly divided with 75% for the calibration set and the remaining 25% for the validation set. The performance of the prediction models was evaluated using the statistic parameters of correlation coefficient of prediction (r_p) and root mean square error of prediction (RMSEP).

RESULTS AND DISCUSSION

Statistics of Measured Quality Parameters

The statistical data of SSC, firmness (slope, FF, Max.F), and color (L*, a*, b*, C*, and H°) for all tested apples are summarized

in **Table 1**. There was no relatively large variation for all the nine quality indexes based on the standard deviation (SD) and coefficient of variation (CV), since all the 140 apples were purchased from the same batch with similar properties. It was observed that the distributions of apple SSC and color were relatively narrow than the firmness, with the CV values close to or smaller than 10%. This observation brought great challenges for predicting SSC and color parameters, which will be discussed in the following section.

Correlations among the SSC, firmness, and color parameters for all apples are summarized in **Table 2**. It was observed that the overall correlation among these quality parameters was not strong, with most of the coefficients smaller than 0.50. This might be due to the fact that the apples used in this study were similar in appearance and had no difference in maturation stage or shelf life, thus causing narrow distribution of quality attributes. It should be noted that the correlation coefficient between the Max.F and FF was as high as 0.80, because the FF was defined as the average force over the puncture distances between the rupture point (Max.F) and puncture depth. This phenomenon was also reported by Huang et al. (2018) when studying tomato fruit based on spatially resolved spectroscopy. The correlation coefficient between b* and C* was 1.00, because the two parameters were very close to each other.

Optical Property Mappings of Apples

To determine the optical property mappings of apples, the TP-CF method was carried out, and the resulting absorption and scattering properties are displayed in **Figures 4A,B**, respectively. The numbers labeled below the sub-pictures are the average values of μ_a or μ_s' for the marked ROI with the size of 30 × 30 pixels. It should be noted that the circular part is sliced apple tissue with relatively flat surface, while the surrounding part, which has a more uniform color distribution, is the sample holder made of aluminum material with blackening treatment. There was a decreased tendency of the μ_a and μ_s' along the four wavelengths. Comparing the scattering properties at a wavelength, like 527 nm in **Figure 4B**, a spatial variation of μ_s' for the apple tissue between 0.996 and 1.152 mm^{-1} was noticed. The complex apple tissue formed by different components with different physicochemical characteristics and the performance of structured illumination (e.g., non-uniformity), as well as data processing algorithm for optical property estimation, are the potential factors that cause the variation. A similar variation also occurs for the μ_a mappings in **Figure 4A**. It was observed that the spatial variation of optical properties at 710 nm was less pronounced than the other three wavelengths, which demonstrates that wavelength plays a non-negligible role when estimating apple optical properties.

Figure 5 shows the average optical properties of four different ROI with the sizes of 10 × 10, 30 × 30, 60 × 60, and 100 × 100 along the four wavelengths. The μ_a and μ_s' for different sizes of ROI are quite similar, but still, a difference can be observed. In general, the optical property value in small size ROI (10 × 10) was slightly different from the value in large size ROI, which might be caused by the spatial variation mentioned above. For the three larger ROIs, the average optical properties were close to each other, with the differences of 6.94–19.0% and 1.56–3.51% for μ_a and μ_s', respectively. Considering the fact that larger-size ROI means more cost of time, the ROI with the size of 30 × 30 was chosen for averaging the μ_a and μ_s' and would be used in the following sections.

To our knowledge, this is the first time that the optical properties of apple tissue were determined from different sizes of ROI. Based on SFDI measurements of "Braeburn" apples, Lohner et al. (2021) recently observed that μ_a was about 0.01–0.04 mm^{-1} for the cortex tissue at 656 nm, which covers the μ_a range at 630 nm in this study (0.021–0.024 mm^{-1}), if the value from the ROI of 10 × 10 is excluded. As known from the previous work, the wavelength of 656 nm is mainly related to the presence of chlorophyll *b* (Merzlyak and Solovchenko, 2002), and it is thus reasonable that the μ_a value is larger than the present results. Our results are also comparable to the published integrating sphere measurements by other researchers. For example, Wei et al. (2020) measured the optical properties of cold-stored "Fuji" apples over 400–1,100 nm and reported that the μ_a was in the range of about 0.02–0.13 mm^{-1}, whereas the μ_s' was between 1.0 and 1.75 mm^{-1} for the flesh tissue, which are comparable with the present results.

TABLE 2 | Pearson's linear correlation coefficients among apple quality parameters.

Parameter	SSC	Slope	FF	Max.F	L*	a*	b*	C*	H°
SSC	1.00								
Slope	0.46	1.00							
FF	**0.51**	0.38	1.00						
Max.F	**0.69**	**0.51**	**0.80**	1.00					
L*	0.32	0.36	0.36	0.36	1.00				
a*	**0.77**	−0.45	−0.32	0.31	−0.48	1.00			
b*	**0.51**	0.48	0.42	**0.53**	**−0.50**	**−0.50**	1.00		
C*	0.49	0.48	0.42	**0.52**	−0.49	**−0.52**	**1.00**	1.00	
H°	**−0.86**	0.38	−0.34	−0.40	**0.57**	**−0.91**	−0.49	−0.46	1.00

Significant correlations are in bold (n = 140, r ≥ 0.5, p-value ≤ 0.05).
SSC, soluble solid content; FF, flesh firmness; Max.F, maximum force.

Correlations Between Optical Properties and Apple Quality Attributes

Table 3 presents the relationships between the average optical properties and apple quality parameters. The correlations between the optical properties and their combinations at 527 and 630 nm measured by SFDI and apple quality parameters are not reported as non-significant. Better correlations were observed between μ_a and quality parameters, compared with μ_s', which is in general agreement with the previous studies for apples, tomatoes, and peaches (Do Trong et al., 2014; Huang et al., 2018; Sun Y. et al., 2020). The μ_{a_460} was negatively related to a* and C* and positively related to b*, slope, FF, and Max.F, whereas μ_{a_710} was only positively related to b* and negatively related to a*, C*, slope, FF, and Max.F. As for scattering, no significant correlations were found between $\mu_s'_{\_460}$ and quality parameters, whereas $\mu_s'_{\_710}$ was positively

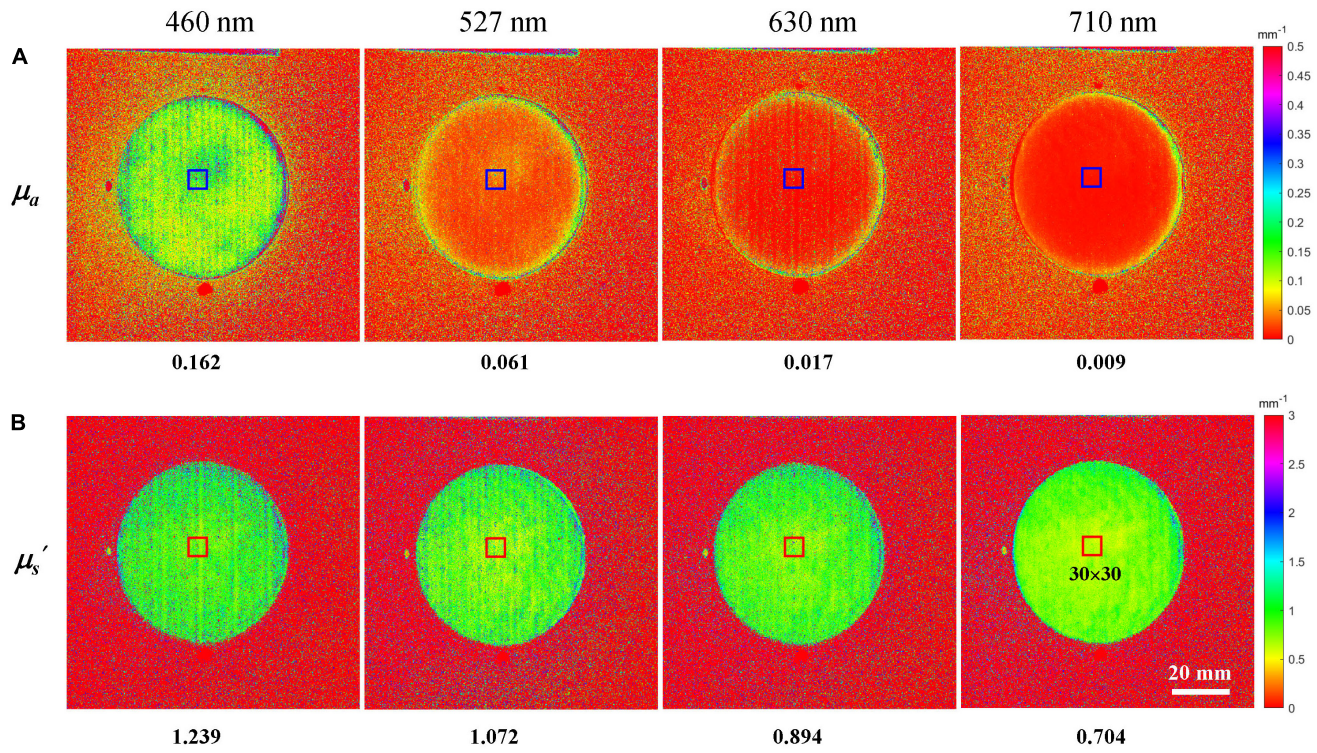

FIGURE 4 | Absorption coefficient **(A)** and reduced scattering coefficient **(B)** mappings of a representative apple at the wavelengths of 460, 527, 630, and 710 nm.

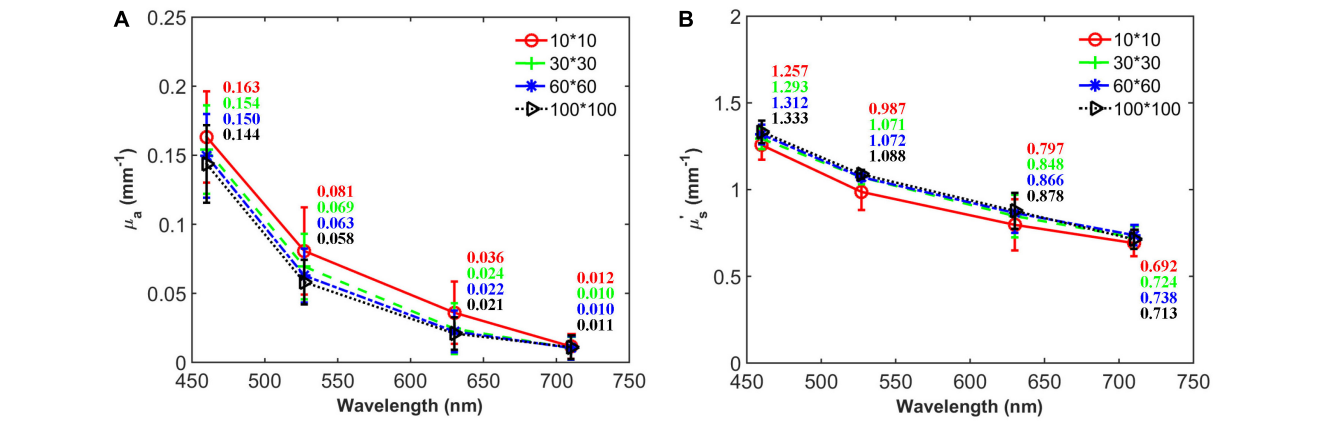

FIGURE 5 | Average absorption coefficient **(A)** and reduced scattering coefficient **(B)** of a representative apple with different sizes of ROI at the wavelengths of 460, 527, 630, and 710 nm.

and negatively related to b* and C*, respectively. It was observed that the combinations of $\mu_a \times \mu_s'\_460$, $\mu_a \times \mu_s'\_710$, μ_{eff}_460, and μ_{eff}_710 resulted in better correlation results, compared with the individual optical properties. This is especially true for the correlations between the color parameters of a*, b*, C*, and $\mu_a \times \mu_s'\_460$, $\mu_a \times \mu_s'\_710$. For example, using $\mu_a \times \mu_s'\_710$ improved correlation coefficients of a*, b*, and C* by 14.8, 25.4, and 25.4%, compared with the correlation analysis based on the μ_a_710. Moreover, a noticeable improvement was found for SSC when using the combinations of optical properties (**Table 3**). These results demonstrated that optical property measurement can provide useful information about the apple quality.

Prediction for Apple Quality Attributes

The resulting r_p and RMSEP from SVM, MLR, and PLS based on μ_a, μ_s', $\mu_a \times \mu_s'$, and μ_{eff} are summarized in **Table 4**. Overall, the prediction result performs not well with the r_p-values of 0.24–0.86 and 0.19–0.82 for the SVM and MLR, respectively. The result predicted by PLS is worse and not reported. It could be

TABLE 3 | Pearson's linear correlation coefficients between optical properties and apple quality parameters.

	μ_a_460	μ_a_710	μ_s'_460	μ_s'_710	$\mu_a \times \mu_s'$_460	$\mu_a \times \mu_s'$_710	μ_{eff}_460	μ_{eff}_710
SSC	−0.42	−0.45	−0.31	−0.39	**−0.61**	**−0.65**	**−0.61**	**−0.64**
Slope	**0.64**	**−0.55**	0.40	0.45	**0.63**	**−0.52**	**0.64**	**−0.53**
FF	**0.61**	**−0.56**	0.33	0.34	**0.69**	**−0.65**	**0.69**	**−0.65**
Max.F	**0.62**	**−0.59**	0.40	0.38	**0.62**	**−0.60**	**0.63**	**−0.59**
L*	0.39	0.32	0.21	0.32	0.49	0.37	0.30	0.28
a*	**−0.57**	**−0.54**	−0.23	−0.20	**−0.65**	**−0.62**	**−0.57**	**−0.61**
b*	**0.59**	**0.59**	0.32	**0.52**	**0.67**	**0.74**	**0.60**	**0.67**
C*	**−0.59**	**−0.59**	−0.32	**−0.52**	**−0.67**	**−0.74**	**−0.60**	**−0.66**
H°	0.36	0.26	0.15	0.11	0.45	**0.50**	0.26	0.28

Significant correlations are in bold (n = 140, r ≥ 0.5, p-value ≤ 0.05).
SSC, soluble solid content; FF, flesh firmness; Max.F, maximum force.

observed that color parameters of b* and C* achieved the best prediction performance (r_p = 0.86), followed by the firmness parameters with the r_p-values of 0.68, 0.73, and 0.79 for slope, FF, and Max.F, and finally, SSC was the most challenging for the prediction (r_p = 0.66). The prediction results for all the apple quality parameters based on μ_a were far better than that based on μ_s', which is consistent with the findings of Pearson's correlation analysis above. The combinations of $\mu_a \times \mu_s'$ and μ_{eff} gave better prediction results, compared to the individual μ_a or μ_s'. For example, using $\mu_a \times \mu_s'$ for predicting the parameter of slope by the SVM resulted in r_p of 0.68, which represents 17.2% improvement, compared with the individual μ_a. It should be mentioned that the combinations improved the prediction of SSC significantly (> 34.0%), which also agrees well with the correlation analysis.

DISCUSSION

Optical property measurement, as a powerful tool for interpreting light-tissue interaction, as well as an alternative solution for quality assessment of plant and food products by quantitatively separating absorption and scattering information from spectroscopic and/or image signals, has received increasing interests. Many fruits and vegetables, such as apple, pear, peach, citrus fruit, tomato, onion, and sweet potato, have been tested using diverse optical measurement techniques (Hu et al., 2015, 2020b; Lu et al., 2020). However, most of the efforts were made to obtain the optical property of single point (usually one pixel in the tissue). To our knowledge, SFDI is the sole technique which is capable of measuring the optical property mappings (in the axial and transverse directions), and till now, only apple and pear fruit have been studied (Hu et al., 2020a; He et al., 2021; Lohner et al., 2021). The apple flesh, as a relatively uniform tissue, should present homogeneous optical property mapping, which was confirmed by the results observed in this paper. For non-uniform samples, such as apple with peel, optical property mapping is critical to elaborate the spatial distribution of optical properties, which, in turn, would help to select the optimal location in optical inspection for quality evaluation.

It is well known that there are several peaks in apple absorbance spectra, which can be attributed to carotenoids around 500 nm, chlorophyll around 670 nm, and water around 980 nm (Vanoli et al., 2020). The wavelengths of 460 and 710 nm, under which better correlations between the optical properties and apple quality parameters were obtained, are close to the absorption peaks of carotenoids and chlorophyll, respectively. However, apple preparation in this study is destructive by removing a slice of about 15 mm, and the color parameters are all measured from the flesh tissues. Though pigments could contribute to flesh coloration, the amounts of carotenoids and chlorophylls in the flesh are very low (Delgado-Pelayo et al., 2014), which could partly explain why the correlations between optical property and color parameters were not high enough.

TABLE 4 | SVM and MLR prediction results for apple quality parameters based on absorption coefficient (μ_a), reduced scattering coefficient (μ_s'), and their combinations.

Quality parameter	Statistic parameter	SVM prediction				MLR prediction			
		μ_a	μ_s'	$\mu_a \times \mu_s'$	μ_{eff}	μ_a	μ_s'	$\mu_a \times \mu_s'$	μ_{eff}
SSC	r_p	0.47	0.30	0.66	0.63	0.40	0.31	0.59	0.60
	RMSEP	1.28	1.27	1.28	1.28	1.32	1.34	1.32	1.32
Slope	r_p	0.58	0.32	0.68	0.67	0.54	0.27	0.60	0.61
	RMSEP	1.65	1.63	1.66	1.66	1.70	1.72	1.71	1.71
FF	r_p	0.64	0.24	0.73	0.72	0.53	0.20	0.63	0.62
	RMSEP	2.24	2.29	2.24	2.25	2.25	2.29	2.25	2.25
Max.F	r_p	0.72	0.25	0.79	0.78	0.56	0.21	0.64	0.64
	RMSEP	1.20	1.27	1.21	1.22	1.28	1.31	1.29	1.29
L*	r_p	0.34	0.35	0.41	0.42	0.31	0.33	0.38	0.40
	RMSEP	1.06	1.01	1.07	1.07	1.09	1.09	1.10	1.10
a*	r_p	0.57	0.35	0.66	0.57	0.52	0.28	0.58	0.50
	RMSEP	0.84	0.82	0.84	0.84	0.86	0.85	0.87	0.87
b*	r_p	0.80	0.61	0.85	0.86	0.75	0.57	0.78	0.82
	RMSEP	2.32	2.42	2.16	2.28	2.52	2.53	2.35	2.44
C*	r_p	0.81	0.61	0.85	0.86	0.75	0.58	0.77	0.82
	RMSEP	2.32	2.42	2.16	2.28	2.53	2.53	2.35	2.44
H°	r_p	0.33	0.26	0.38	0.37	0.31	0.19	0.33	0.32
	RMSEP	1.73	1.71	1.70	1.71	1.76	1.78	1.75	1.76

SSC, soluble solid content; FF, flesh firmness; Max.F, maximum force; r_p, correlation coefficient of prediction; RMSEP, root mean square error of prediction.

This study showed that absorption properties provided useful information for apple SSC, firmness, and color prediction, while the prediction performance based on the scattering properties was much worse. This observation is general agreement with the previous studies for apple, peach, and tomato using the spatially resolved technique (Do Trong et al., 2014; Huang et al., 2018; Sun Y. et al., 2020). For SSC and color parameters, they are closely related to the chemical compositions and pigment contents in apples, which have direct relationships with the absorption properties. On the other hand, and surprisingly enough, the prediction of firmness parameters based on the absorption properties was far better than that based on the scattering properties. This unexpected outcome could be attributed to the fact that SFDI is limited to light penetration depth (2–3 mm) (Lu and Lu, 2019; Hu et al., 2021), while the firmness measurement by the texture analyzer probed the flesh much deeper (8 mm). In addition, the wavelengths used in this study are near to the characteristic wavelengths with absorption peaks, while the scattering properties have no features in those wavelengths. This may also explain why absorption properties performed better correlations with apple quality parameters than scattering properties. Since the apple quality is accompanied with both chemical compositions and tissue microstructures, the combinations of optical properties could improve the prediction performance.

The prediction models based on SVM were superior to the models established by MLR and PLS. This may be attributed to the fact that four wavelengths are not adequate to establish the stable and adaptable MLR and PLS models, while SVM is one of machine-learning methods, which is more powerful in dealing with this issue. This observation suggests that other machine-learning and deep learning methods, such as artificial neural network and convolutional neural network, can be tested for quality prediction based on optical properties in the future. Overall, the correlation and prediction performance between the optical properties and quality parameters were comparable to the results of some published work. For instance, He et al. (2016) and Sun C. et al. (2020) showed that the prediction models for SSC of pear and citrus fruit based on the μ_a spectra measured by integrating sphere technique gave the r_p-values of 0.63 and 0.67, respectively, while the r_p for SSC of tomato fruit based on the absorption properties estimated from spatially resolved diffuse reflectance was 0.62 (Huang et al., 2018), which are all comparable to the r_p of 0.66 in this study. As for the firmness prediction, He et al. (2016) reported that the PLS model gave r_p-value of 0.66, which was less satisfied than the results of Do Trong et al. (2014) (r_p = 0.84). The apple color prediction in this study was much better than the result reported by Vanoli et al. (2020) based on time- and spatially resolved techniques. Though the prediction performance of these results showed great differences, which may be in part caused by the factors of cultivar, growing, maturity and storage conditions, and measuring technique, they all demonstrated that there was a great potential for quality prediction based on the measured optical properties. However, in this paper, the results are still far away from practical application in the field of non-destructive inspection. Very few samples and characteristic wavelengths, as well as the narrow distribution of quality attributes (SSC, firmness, and color) for the apple samples used in this study, are the critical factors that result in low r_p-values. Furthermore, relatively low correlation for SSC could also be caused by the different locations (i.e., the left and right pieces in **Figure 1**) for juicing and SFDI measurements. Apples were cut into two parts in the sample preparation to generate a relatively smooth surface, which is critical to keep the distance between camera and sample surface consistent during SFDI measurement. However, this operation could not meet the requirement of non-destructive inspection in practical applications. Apple contour has non-negligible effect on optical property mapping, and thus, the contour correction is worth studying in the future research.

CONCLUSION

The optical property mappings of "Golden Delicious" apples were measured using the SFDI technique at the wavelengths of 460, 527, 630, and 710 nm. Spatial variations in the absorption coefficient (μ_a) and reduced scattering coefficient (μ_s') mappings for the sliced flesh tissue were noticed, but overall, the μ_a and μ_s' distributions were relatively uniform. Different sizes of ROI (10 × 10, 30 × 30, 60 × 60, and 100 × 100 pixels) had less effect on the average μ_a and μ_s', except for the 10 × 10 that was too small. The average μ_a and μ_s' showed a decreased tendency along the four wavelengths. Correlations between apple quality parameters and μ_a and μ_s', as well as their combinations ($\mu_a \times \mu_s'$ and μ_{eff}) at 460 and 710 nm, were superior to those at 527 and 630 nm, since the former two wavelengths were close to the absorption peaks. The prediction for quality parameters (SSC, firmness, and color) based on the μ_a was far better than that based on the μ_s', and the combinations of $\mu_a \times \mu_s'$ and μ_{eff} improved the prediction performance, compared to the individual μ_a or μ_s'. The prediction models established based on SVM outperformed those by MLR and PLS. The best prediction models for SSC, slope, FF, and Max.F were all achieved based on the $\mu_a \times \mu_s'$, with the correlation coefficients of prediction (r_p) of 0.66, 0.68, 0.73, and 0.79, respectively, whereas the μ_{eff} gave the best prediction for most of the color parameters, with the r_p-value of 0.86 for both of the parameters of b* and C*.

DATA AVAILABILITY STATEMENT

The original contributions presented in the study are included in the article/supplementary material, further inquiries can be directed to the corresponding author/s.

AUTHOR CONTRIBUTIONS

HP: conceptualization, data analysis, writing, reviewing, editing, and project administration. CZ: data collection,

methodology, reviewing, and editing. ZS: data analysis, reviewing, and editing. TS and JW: reviewing and editing. DH: conceptualization, methodology, data collection, final analysis, writing—original draft preparation, reviewing, and editing. ZY: resources, reviewing, and editing. All authors contributed to the article and approved the submitted version.

FUNDING

This work was supported by Zhejiang Basic Public Welfare Research Project (grant no. LGN18B060001), the Natural Science Foundation of Zhejiang Province (grant no. LQ20C130002), and the National Natural Science Foundation of China (grant no. 32001414).

REFERENCES

Daniels, A. J., Poblete-Echeverría, C., Nieuwoudt, H. H., Botha, N., and Opara, U. L. (2021). Classification of browning on intact table grape bunches using near-infrared spectroscopy coupled with partial least squares-discriminant analysis and artificial neural networks. *Front. Plant Sci.* 12:768046. doi: 10.3389/fpls.2021.768046

Delgado-Pelayo, R., Gallardo-Guerrero, L., and Hornero-Méndez, D. (2014). Chlorophyll and carotenoid pigments in the peel and flesh of commercial apple fruit varieties. *Food Res. Int.* 65, 272–281. doi: 10.1016/j.foodres.2014.03.025

Do Trong, N. N., Erkinbaev, C., Tsuta, M., De Baerdemaeker, J., Nicolaï, B., and Saeys, W. (2014). Spatially resolved diffuse reflectance in the visible and near-infrared wavelength range for non-destructive quality assessment of 'Braeburn'apples. *Postharv. Biol. Technol.* 91, 39–48. doi: 10.1016/j.postharvbio.2013.12.004

Fan, S., Wang, Q., Tian, X., Yang, G., Xia, Y., Li, J., et al. (2020). Non-destructive evaluation of soluble solids content of apples using a developed portable Vis/NIR device. *Biosyst. Eng.* 193, 138–148. doi: 10.1016/j.biosystemseng.2020.02.017

Flock, S. T., Wilson, B. C., and Patterson, M. S. (1987). Total attenuation coefficients and scattering phase functions of tissues and phantom materials at 633 nm. *Med. Phys.* 14, 835–841. doi: 10.1118/1.596010

Gao, F., Dong, Y., Xiao, W., Yin, B., Yan, C., and He, S. (2016). LED-induced fluorescence spectroscopy technique for apple freshness and quality detection. *Postharv. Biol. Technol.* 119, 27–32. doi: 10.1016/j.postharvbio.2016.04.020

Gigan, S. (2017). Optical microscopy aims deep. *Nat. Phot.* 11, 14–16. doi: 10.1038/nphoton.2016.257

Hayakawa, C. K., Karrobi, K., Pera, V. E., Roblyer, D. M., and Venugopalan, V. (2018). Optical sampling depth in the spatial frequency domain. *J. Biomed. Opt.* 24:071603. doi: 10.1117/1.JBO.24.7.071603

He, X., Fu, X., Rao, X., and Fang, Z. (2016). Assessing firmness and SSC of pears based on absorption and scattering properties using an automatic integrating sphere system from 400 to 1150 nm. *Postharv. Biol. Technol.* 121, 62–70. doi: 10.1016/j.postharvbio.2016.07.013

He, X., Hu, D., Fu, X., and Rao, X. (2021). Spatial frequency domain imaging for determining absorption and scattering properties of bruised pears based on profile corrected diffused reflectance. *Postharv. Biol. Technol.* 179:111570. doi: 10.1016/j.postharvbio.2021.111570

Hu, D., Fu, X., He, X., and Ying, Y. (2016). Noncontact and wide-field characterization of the absorption and scattering properties of apple fruit using spatial-frequency domain imaging. *Sci. Rep.* 6:37920. doi: 10.1038/srep37920

Hu, D., Fu, X., Wang, A., and Ying, Y. (2015). Measurement methods for optical absorption and scattering properties of fruits and vegetables. *Trans. ASABE* 58, 1387–1401. doi: 10.13031/trans.58.11103

Hu, D., Huang, Y., Zhang, Q., Yao, L., Yang, Z., and Sun, T. (2021). Numerical simulation on spatial-frequency domain imaging for estimating optical absorption and scattering properties of two-layered horticultural products. *Appl. Sci.* 11:617. doi: 10.3390/app11020617

Hu, D., Lu, R., and Ying, Y. (2018). A two-step parameter optimization algorithm for improving estimation of optical properties using spatial frequency domain imaging. *J. Quantit. Spectrosc. Radiat. Transfer* 207, 32–40. doi: 10.1016/j.jqsrt.2017.12.022

Hu, D., Lu, R., and Ying, Y. (2020a). Spatial-frequency domain imaging coupled with frequency optimization for estimating optical properties of two-layered food and agricultural products. *J. Food Eng.* 277:109909. doi: 10.1016/j.jfoodeng.2020.109909

Hu, D., Sun, T., Yao, L., Yang, Z., Wang, A., and Ying, Y. (2020b). Monte Carlo: A flexible and accurate technique for modeling light transport in food and agricultural products. *Trends Food Sci. Technol.* 102, 280–290. doi: 10.1016/j.tifs.2020.05.006

Hu, D., Lu, R., Ying, Y., and Fu, X. (2019). A stepwise method for estimating optical properties of two-layer turbid media from spatial-frequency domain reflectance. *Opt. Expr.* 27, 1124–1141. doi: 10.1364/OE.27.001124

Huang, Y., Lu, R., and Chen, K. (2020). Detection of internal defect of apples by a multichannel Vis/NIR spectroscopic system. *Postharv. Biol. Technol.* 161:111065. doi: 10.1016/j.postharvbio.2019.111065

Huang, Y., Lu, R., Hu, D., and Chen, K. (2018). Quality assessment of tomato fruit by optical absorption and scattering properties. *Postharv. Biol. Technol.* 143, 78–85. doi: 10.1016/j.postharvbio.2018.04.016

Li, J., and Zhang, Z. (2021). *Nondestructive Evaluation of Agro-Products by Intelligent Sensing Techniques*. Sharjah: Bentham Science Publishers.

Lohner, S. A., Biegert, K., Nothelfer, S., Hohmann, A., McCormick, R., and Kienle, A. (2021). Determining the optical properties of apple tissue and their dependence on physiological and morphological characteristics during maturation. *Part 1: Spat. Frequency Domain Imaging. Postharvest Biol. Technol.* 181:111647. doi: 10.1016/j.postharvbio.2021.111647

Lu, R., Van Beers, R., Saeys, W., Li, C., and Cen, H. (2020). Measurement of optical properties of fruits and vegetables: A review. *Postharvest Biol. Technol.* 159:111003. doi: 10.1016/j.postharvbio.2019.111003

Lu, Y., Li, R., and Lu, R. (2016). Fast demodulation of pattern images by spiral phase transform in structured-illumination reflectance imaging for detection of bruises in apples. *Comput. Electr. Agricult.* 127, 652–658. doi: 10.1016/j.compag.2016.07.012

Lu, Y., and Lu, R. (2019). Structured-illumination reflectance imaging for the detection of defects in fruit: analysis of resolution, contrast and depth-resolving features. *Biosyst. Eng.* 180, 1–15. doi: 10.1016/j.biosystemseng.2019.01.014

Merzlyak, M. N., and Solovchenko, A. E. (2002). Photostability of pigments in ripening apple fruit: a possible photoprotective role of carotenoids during plant senescence. *Plant Sci.* 163, 881–888. doi: 10.1016/S0168-9452(02)00241-8

Sun, C., Van Beers, R., Aernouts, B., and Saeys, W. (2020). Bulk optical properties of citrus tissues and the relationship with quality properties. *Postharvest Biol. Technol.* 163:111127. doi: 10.1016/j.postharvbio.2020.111127

Sun, Y., Lu, R., and Wang, X. (2020). Evaluation of fungal infection in peaches based on optical and microstructural properties. *Postharvest Biology and Technol.* 165:111181. doi: 10.1016/j.postharvbio.2020.111181

Sun, Z., Hu, D., Xie, L., and Ying, Y. (2022). Detection of early stage bruise in apples using optical property mapping. *Comput. Electr. Agricult.* 194:106725. doi: 10.1016/j.compag.2022.106725

Sun, Z., Xie, L., Hu, D., and Ying, Y. (2021). An artificial neural network model for accurate and efficient optical property mapping from spatial-frequency domain images. *Comput. Electr. Agricult.* 188:106340. doi: 10.1016/j.compag.2021.106340

Tian, X., Wang, Q., Huang, W., Fan, S., and Li, J. (2020). Online detection of apples with moldy core using the Vis/NIR full-transmittance spectra. *Postharvest Biol. Technol.* 168:111269. doi: 10.1016/j.postharvbio.2020.111269

van Wyngaard, E., Blancquaert, E., Nieuwoudt, H., and Aleixandre-Tudo, J. L. (2021). Infrared spectroscopy and chemometric applications for the qualitative and quantitative investigation of grapevine organs. *Front. Plant Sci.* 12:723247. doi: 10.3389/fpls.2021.723247

Vanoli, M., Van Beers, R., Sadar, N., Rizzolo, A., Buccheri, M., Grassi, M., et al. (2020). Time-and spatially-resolved spectroscopy to determine the bulk optical

properties of 'Braeburn'apples after ripening in shelf life. *Postharvest Biol. Technol.* 168:111233. doi: 10.1016/j.postharvbio.2020.111233

Wan, L., Zhu, J., Du, X., Zhang, J., Han, X., Zhou, W., et al. (2021). A model for phenotyping crop fractional vegetation cover using imagery from unmanned aerial vehicles. *J. Exp. Bot.* 72, 4691–4707. doi: 10.1093/jxb/erab194

Wei, K., Ma, C., Sun, K., Liu, Q., Zhao, N., Sun, Y., et al. (2020). Relationship between optical properties and soluble sugar contents of apple flesh during storage. *Postharvest Biol. Technol.* 159:111021. doi: 10.1016/j.postharvbio.2019.111021

Zhang, Z., Igathinathane, C., Li, J., Cen, H., Lu, Y., and Flores, P. (2020). Technology progress in mechanical harvest of fresh market apples. *Comput. Electr. Agricult.* 175:105606. doi: 10.1016/j.compag.2020.105606

Zhang, Z., Lu, Y., and Lu, R. (2021). Development and evaluation of an apple infield grading and sorting system. *Postharvest Biol. Technol.* 180:111588. doi: 10.1016/j.postharvbio.2021.111588

Zhao, Y., Chu, B., Fang, S., Zhao, J., Zhang, H., and Yu, K. (2020). Potential of vibrational spectroscopy for rapid and accurate determination of the hydrogen peroxide treatment of plant leaves. *Spectrochim. Acta Part A: Mol. Biomol. Spectrosc.* 230:118048. doi: 10.1016/j.saa.2020.118048

Conflict of Interest: The authors declare that the research was conducted in the absence of any commercial or financial relationships that could be construed as a potential conflict of interest.

Publisher's Note: All claims expressed in this article are solely those of the authors and do not necessarily represent those of their affiliated organizations, or those of the publisher, the editors and the reviewers. Any product that may be evaluated in this article, or claim that may be made by its manufacturer, is not guaranteed or endorsed by the publisher.